Chapter 2
Circular Dichroism Spectroscopy with the SAC-CI Methodology: A ChiraSac Study

Tomoo Miyahara and Hiroshi Nakatsuji

Abstract Circular dichroism (CD) spectroscopy reflects sensitively the various chemistries involved in chiral molecules and molecular systems. The CD spectra are very sensitive to the conformational changes of molecules: the rotation around the single bond including a chiral atom. It is also sensitive to the changes in the stacking interactions in the chiral DNA and RNA. Since these changes are low-energy processes, we expect that the CD spectra include a lot of information of the chiral molecular systems. On the other hand, the SAC-CI method is a highly reliable excited-state theory and gives very reliable theoretical CD spectra. Therefore, by comparing the experimental CD spectra with the theoretical SAC-CI spectra calculated for various chemical situations, one can study various chemistries such as the nature of the weak interactions involved in chiral molecular systems and biology. Based on these facts, we are developing a new molecular technology called ChiraSac, a term combining chirality and SAC-CI, to study chiral molecular systems and the chemistry involved thereof. We utilize highly reliable SAC-CI method together with many useful quantum chemical methods involved in Gaussian suite of programs. In this chapter, we review our ChiraSac studies carried out to clarify the chemistries of some chiral molecules and molecular systems: large dependences of the CD spectra on the conformations of several chiral molecules in solutions and the effects of the stacking interactions of the nuclear-acid bases in DNA and RNA on the shapes of their CD spectra. The results of our several studies show that the ChiraSac is a useful tool for studying the detailed chemistry involved in chiral molecular and biological systems.

Keywords Chirality · Circular dichroism spectra · SAC-CI theory · Sensitivity on low-energy processes · Conformational dependence · Stacking interaction · DNA · RNA

T. Miyahara · H. Nakatsuji (✉)
Quantum Chemistry Research Institute, Kyoto Technoscience Center 16, 14 Yoshida-Kawara-Machi, Sakyou-ku, Kyoto 606-8305, Japan
e-mail: h.nakatsuji@qcri.or.jp

M.J. Wójcik et al. (eds.), *Frontiers of Quantum Chemistry*,
https://doi.org/10.1007/978-981-10-5651-2_2

2.1 Introduction

The symmetry adapted cluster (SAC)/SAC—configuration interaction (SAC-CI) [1–6] method proposed by Nakatsuji and Hirao in 1978 is one of the most reliable excited-state theories. Figure 2.1 explains the subjects of the SAC/SAC-CI program available in Gaussian program. SAC is an accurate coupled-cluster theory for ground state, and SAC-CI is the theory for the excited, ionized, and electron-attached states produced from the ground state calculated by the SAC theory. The energy gradient method that calculates the forces acting on the nuclei of molecules facilitates the studies of the molecular equilibrium geometries and dynamics among various electronic states [7–13]. The SAC/SAC-CI code was released in 2003 through Gaussian suite of programs [14] and has been applied to various chemistry and physics involving various electronic sates, ground and excited states from singlet to septet spin multiplicities as shown in Fig. 2.1 [15–20].

In this review, we focus on the application of the SAC/SAC-CI theory and program to the chiral world of chemistry and biology. Chirality is caused by an asymmetric carbon atom that is bonded with four different atoms or groups as shown in Fig. 2.2. In the chiral molecule of Fig. 2.2, since all bonds are single bond and then their rotations around the bond are low-energy processes, the groups (R_1 to R_4) can rotate easily by an external stimulus. Namely, even a weak interaction causes a different conformation. As such weak interaction, solute-solvent interaction, hydrogen-bonding interaction and/or stacking interaction in biological system, etc., are very interesting subject.

The circular dichroism (CD) spectroscopy [21, 22] is one of the most powerful techniques to study chemistry caused by the chirality. Furthermore, the CD spectra are very sensitive to the conformational changes of the chiral molecules [23–35]. Therefore, the CD spectra are used not only for distinguishing the absolute chiral geometries of amino acids, sugars, etc., but also for understanding the nature of the

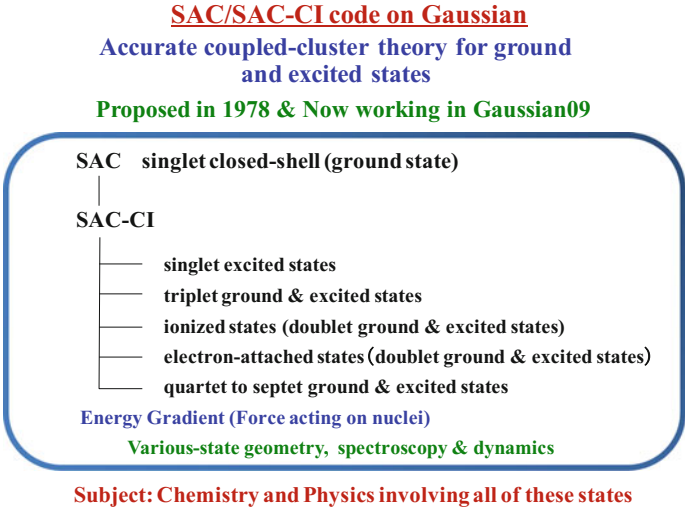

Fig. 2.1 Overview of the SAC-CI program in Gaussian

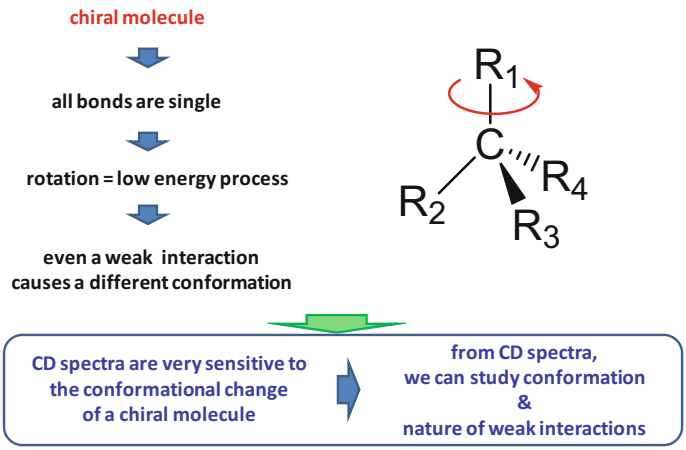

Fig. 2.2 Chiral molecule, conformation and weak interactions

interactions that leads to the observed structures and conformations of the chiral molecules in solution or proteins. Though the UV spectra change only slightly by the change in conformations and/or weak interactions, the CD spectra sometimes change drastically with such changes. Therefore, from the CD spectra, we can obtain much information concerning the nature of weak interactions that are involved in the observed structures and conformations.

Recently, we have applied the SAC/SAC-CI method to the analysis of the CD spectra of various molecules and systems [36–44]. It was confirmed that the CD spectra are very sensitive to the rotations around the single bond of the chiral atom [40–42] and to the weak interactions involved in the chiral DNA and RNA helical structures [40, 43, 44]. Thus, through the CD spectra, we can study the natures of the weak interactions involved in these subjects. However, for such studies, we need a highly reliable theory like the SAC-CI theory to analyze the information involved in the CD spectra. We have confirmed that the SAC-CI method can provide reliable theoretical CD spectra of molecules and molecular systems [36–44]. Based on this fact, we are developing a theoretical methodology, ChiraSac [41–44], to study chemistry involved in chiral molecular systems. Figure 2.3 is an overview of the ChiraSac project. There, we use the SAC-CI method as a central reliable methodology, as well as other useful methods included in the Gaussian suite of program [14] to study the nature of chemistry provided by the CD spectral information on the structure, conformation, interaction with protein environment, solvent effect, etc.

In this review, we introduce some recent studies of the CD spectroscopy with the SAC-CI method. The computational details are described in the reference of each study. First, we discuss the gauge-origin independent method required for the CD spectral calculations [38]. Second, we discuss the conformational dependence of the CD spectra on the rotation around the single bonds involving the chiral atom: the molecule we deal with here is α-hydroxyphenylacetic acid (HPAA) [41] and deoxyguanosine [40]. Third, we discuss the CD spectral change with the substituent

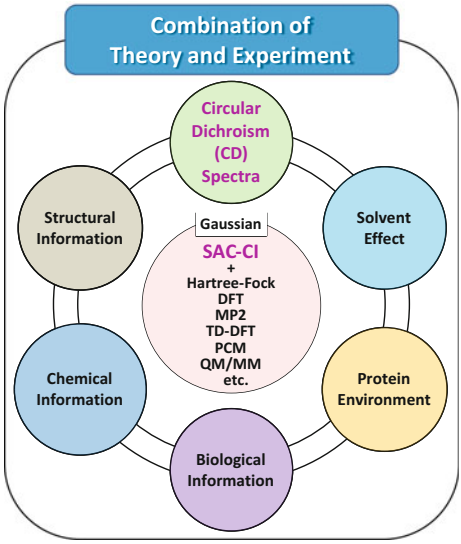

Fig. 2.3 Overview of a ChiraSac project. (Reprinted from Ref. [42] with permission from *The Journal of Physical Chemistry A* **2014**, *118*, 2931–2941. Copyright 2014 American Chemical Society.)

change for the uridine derivatives [42]. Finally, we discuss the weak interactions involved in the CD spectra of the double-helical DNA and RNA [40, 43, 44].

2.2 Rotatory Strength

The intensity of the CD spectra is calculated as the rotatory strength (R_{0a}). It is the imaginary part of the scalar product of the electric and magnetic transition moments between the ground state (Ψ_0) and the excited state (Ψ_a) [45]

$$R_{0a} = \mathrm{Im}\{\langle\Psi_0|\hat{\mu}|\Psi_a\rangle\langle\Psi_a|\hat{m}|\Psi_0\rangle\} \tag{2.1}$$

where $\hat{\mu}$ is an electric dipole moment operator and $\hat{m}$ is a magnetic dipole moment operator. This formula is called the length-gauge expression. The electric transition dipole moment is gauge-origin independent if the ground and excited-state wave functions are orthogonal to each other. On the other hand, the magnetic transition dipole moment is gauge-origin dependent. Using the Hypervirial theorem [46] given by

$$\langle a|\nabla|0\rangle = (E_a - E_0)\langle a|\hat{\mu}|0\rangle, \tag{2.2}$$

Equation (2.1) can be readily transformed to

$$R_{0a} = \mathrm{Im}\left\{\frac{\langle\Psi_0|\nabla|\Psi_a\rangle\langle\Psi_a|\hat{m}|\Psi_0\rangle}{E_a - E_0}\right\}. \tag{2.3}$$

called a velocity form [47], in which the gauge-origin dependent terms cancel each other. Therefore, Eq. (2.3) is gauge-origin independent.

2.3 Gauge-Origin Dependency

The gauge-origin dependency of the rotatory strength was studied for R-methyloxirane calculated by both length and velocity forms (Eqs. (2.1) and (2.3)) [38]. As shown in Table 2.1, when the gauge-origin is at the center of gravity (Z = 0.0 Å calculation), the difference between the length and velocity forms is very small. However, when the gauge-origin is 100.0 Å away from the center of gravity (Z = 100.0 Å calculation), the results of the velocity form are much different from those of the length form. For the 1, 3, and 7^1A excited states, the sign as well as the intensity is different between the two forms for the Z = 100.0 Å calculation. However, for the velocity form, the results of the Z = 100.0 Å calculation are completely the same as those of the Z = 0.0 Å calculation. Therefore, in this review, we will give the results of only the velocity form, because the results of the length form are gauge-origin dependent.

2.4 Dependence of the CD Spectra on the Conformation of HPAA

As described above, the CD spectra of chiral molecules are sensitive to their conformational changes. Since the conformational change is usually a low-energy process, it is difficult to determine its conformation from only the experimental CD

Table 2.1 Gauge-origin dependency of the rotational strength of R-methyloxirane calculated by the length and velocity forms. (Ref. [38])

State	EE (eV)	Osc (au)	Rot.(Z = 0.0 Å)		Rot.(Z = 100.0 Å)		Expt.[a]	
			Length (10^{-40} cgs)	Velocity (10^{-40} cgs)	Length (10^{-40} cgs)	Velocity (10^{-40} cgs)	EE (eV)	RS (10^{-40} cgs)
1^1A	7.02	0.0087	−10.2528	−10.9735	3.8350	−10.9735	7.08	−12.5
2^1A	7.42	0.0100	−0.8958	−1.0157	−2.3484	−1.0157		
3^1A	7.48	0.0158	5.3549	5.2376	−32.0254	5.2376		
4^1A	7.67	0.0112	1.8980	2.1076	18.0443	2.1076	7.70	+5.9
5^1A	7.85	0.0043	6.6438	7.7420	0.8239	7.7420		
6^1A	8.39	0.0047	−0.8264	−1.8091	2.7451	−1.8091		
7^1A	8.44	0.0293	−9.9709	−8.9756	56.5058	−8.9756	8.35	−4.1
8^1A	8.52	0.0020	−4.6979	−4.9544	−23.3448	−4.9544		
9^1A	8.64	0.0060	1.2102	1.3491	3.6837	1.3491		

[a]Ref. [48]

spectrum. However, when we have a reliable theory, we can calculate the CD spectra against the conformational change and we can say the conformation of the molecule from the CD spectra alone by comparing the theoretical CD spectrum with the experimental one. Of course, we can also calculate the stable conformation from the energetic point of view. In this section, we show the conformational dependence of the CD spectra of α-hydroxyphenylacetic acid (HPAA) on the rotations around the single bonds that are low-energy processes [41].

In HPAA, carboxyl (COOH), hydroxyl (OH), and phenyl (C_6H_5) groups are bound to the chiral carbon atom (marked with * in Fig. 2.4) by single bonds. We calculated the potential energy curves for each rotation as a function of the dihedral angles, Δ1, Δ2, or Δ3 taking the optimized angles as 0 degree and the results are shown in Fig. 2.4. At low temperature, only the phenyl rotation is important. However, since the energy barriers are small, the hydroxyl and carboxyl groups can also rotate at high temperature.

Figures 2.5, 2.6 and 2.7 show the SAC-CI CD spectra of HPAA at several conformational angles of the phenyl, COOH, and OH rotations, compared with the experimental CD spectrum (black line) observed at 27 °C [49]. For the CD spectra of HPAA, the lowest excited state is the excitation of HOMO to LUMO (π-π*) of the phenyl group corresponding to the peak at 260 nm and the second excited state is the excitation of the non-bonding orbital to the π* orbital of the COOH group corresponding to the peak at 220 nm.

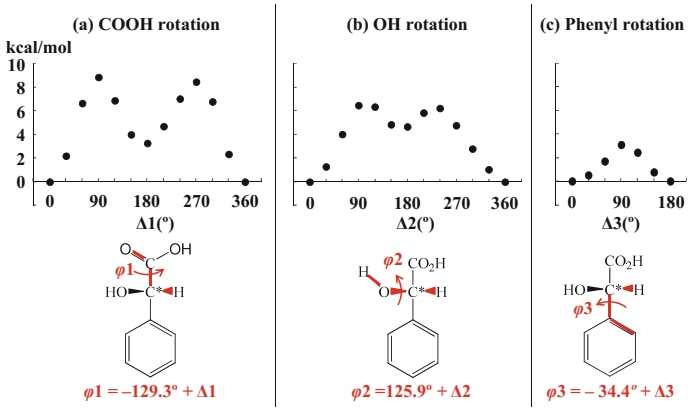

Fig. 2.4 Potential energy curves for the **a** COOH, **b** OH, and **c** phenyl rotations of α-hydroxyphenylacetic acid, as a function of the dihedral angle change (Δ1, Δ2, Δ3) from the fully optimized dihedral angles $\varphi 1 = -129.3$, $\varphi 2 = 125.9$, and $\varphi 3 = -34.4°$. The definition of each dihedral angle is shown by the red lines in each structural formula. (Reprinted from Ref. [41] with permission from *The Journal of Physical Chemistry A* **2013**, *117*, 14065–74. Copyright 2013 American Chemical Society.)

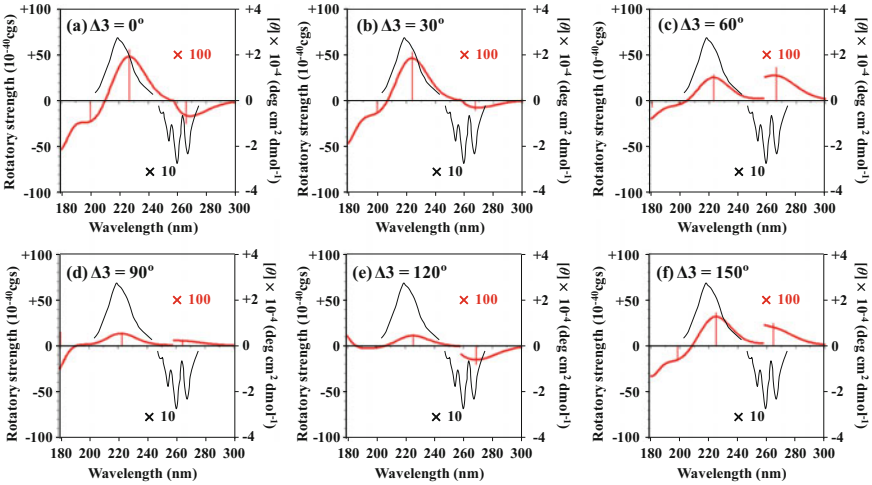

Fig. 2.5 SAC-CI CD spectra (*red lines*) of α-hydroxyphenylacetic acid at several conformational angles of the phenyl rotation, compared with the experimental CD spectrum (*black line* [49]) (Reprinted from Ref. [41] with permission from *The Journal of Physical Chemistry A* **2013**, *117*, 14065–74. Copyright 2013 American Chemical Society.)

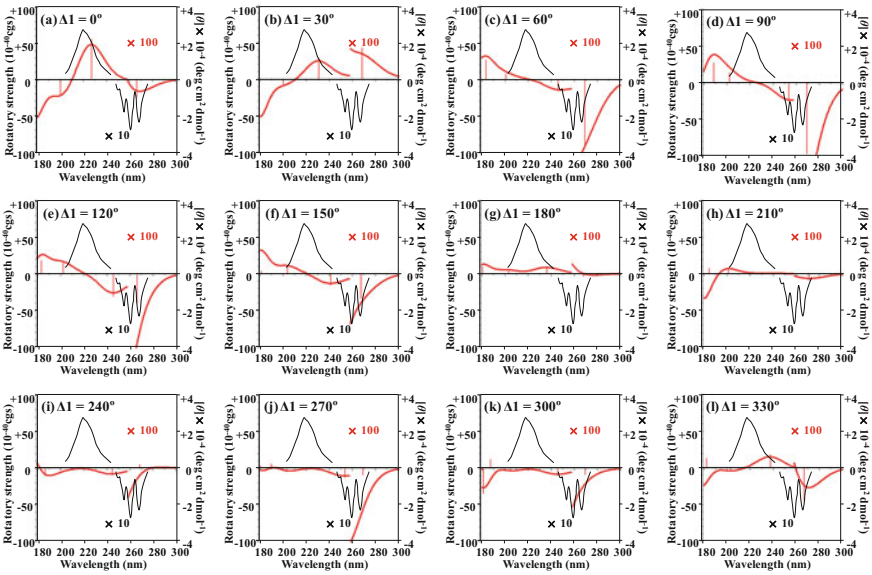

Fig. 2.6 SAC-CI CD spectra (*red lines*) of α-hydroxyphenylacetic acid at several conformational angles of the carboxyl (COOH) rotation, compared with the experimental CD spectrum (*black line* [49]) (Reprinted from Ref. [41] with permission from *The Journal of Physical Chemistry A* **2013**, *117*, 14065–74. Copyright 2013 American Chemical Society.)

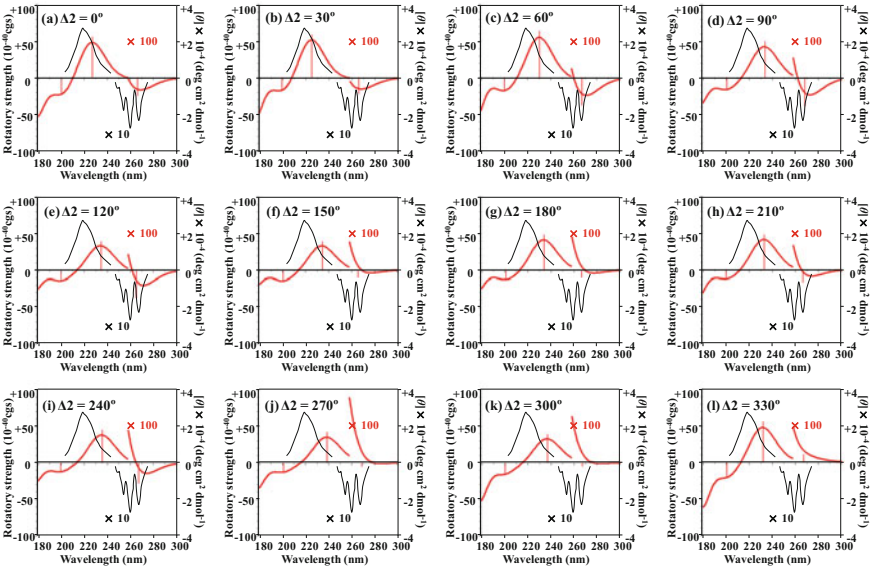

Fig. 2.7 SAC-CI CD spectra (*red lines*) of α-hydroxyphenylacetic acid at several conformational angles of the hydroxyl (OH) rotation, compared with the experimental CD spectrum (*black line* [49]) (Reprinted from Ref. [41] with permission from *The Journal of Physical Chemistry A* **2013**, *117*, 14065–74. Copyright 2013 American Chemical Society.)

For the Phenyl rotation (Fig. 2.5), the first band (phenyl π-π*) largely depends on the phenyl rotation because of the π-π* excitation of the phenyl group. However, the second band is positive for all conformations because of the n-π* excitation of the COOH group.

For the COOH rotation (Fig. 2.6), the first band is negative except for $\Delta 1 = 30°$. However, the sign and intensity of the second band (n-π* of COOH) largely change by the COOH rotation due to the n-π* excitation of the COOH group.

For the OH rotation (Fig. 2.7), the SAC-CI CD spectra are similar to each other among all conformations, because the excitation of the OH group is not included in the 200–300 nm region.

Finally, we calculated the Boltzmann averaged SAC-CI CD spectra of HPAA at several different temperatures shown in Fig. 2.8, considering that the energy barriers around the single bond rotations are relatively low. The SAC-CI CD spectrum at 27 °C (purple line) is similar to the SAC-CI CD spectrum of the most stable conformer (Figs. 2.5a, 2.6a and 2.7a). But, as the temperature increases, the intensity decreases in all regions due to the contribution of the unstable conformers.

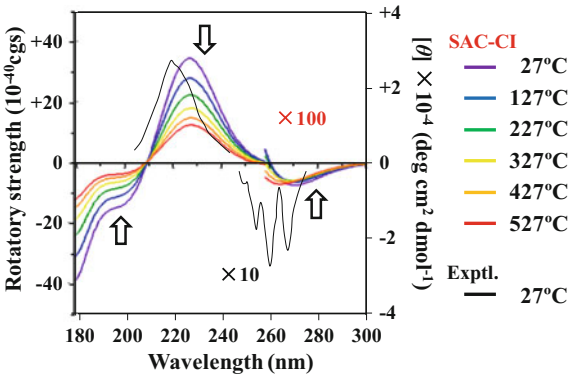

Fig. 2.8 Boltzmann averaged SAC-CI CD spectra of α-hydroxyphenylacetic acid at several different temperatures, compared with the experimental CD spectrum [49]. *Arrows* indicates the directions of the changes caused by raising the temperature (Reprinted from Ref. [41] with permission from *The Journal of Physical Chemistry A* **2013**, *117*, 14065–74. Copyright 2013 American Chemical Society.)

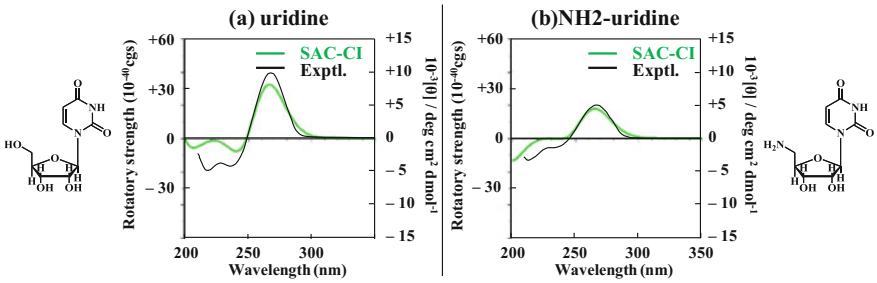

Fig. 2.9 Experimental CD spectra (*black lines*) of uridine and NH2-uridine compared with the SAC-CI CD Boltzmann average spectra (*green lines*) (Reprinted from Ref. [42] with permission from *The Journal of Physical Chemistry A* **2014**, *118*, 2931–2941. Copyright 2014 American Chemical Society.)

2.5 Substituent Effect of Uridine Derivatives

Next, we study the CD spectra of uridine and NH2-uridine shown in Fig. 2.9. NH2-uridine has an NH2 group at the C5' position of the ribose. The intensity of the experimental CD spectrum is strong for uridine but weak for NH2-uridine [50, 51]. The Boltzmann averaged SAC-CI CD spectra of uridine and NH2-uridine are compared with the experimental spectra [50] in Fig. 2.9. The SAC-CI CD spectra successfully reproduced the difference between uridine and NH2-uridine.

The rotatory strength (R_{0a}) of the CD spectra is expressed using the angle θ between the electric transition dipole moment (ETDM, μ) and the magnetic transition dipole moment (MTDM, m) as

$$R_{0a} = \mathrm{Im}[|\vec{\mu}_{0a}||\vec{m}_{0a}| \cos\theta] \tag{2.4}$$

In the most stable anti-conformation, the dihedral angle between uracil and ribose was calculated to be 173.9º for uridine and 176.7º for NH2-uridine. Although the dihedral angle difference is very small, the intensity of the CD spectra is different between uridine and NH2-uridine. The first excited state corresponding to the peak at 267 nm is the n-π* excitation of uracil. However, this state also includes the π-π* excitation of uracil. The ETDM depends on the ratio of the mixing of the π-π* excitation. Since the mixing of the π-π* excitation with the n-π* excitation of uracil is large for uridine but small for NH2-uridine, the ETDM is larger for uridine (0.067) than for NH2-Uridine (0.016). This is the main reason that the intensity of the first peak is weaker for NH2-uridine than for uridine.

For the second excited state of the π-π* excitation that corresponds to the peak at 235 nm, the angle θ of NH2-uridine is closer to 90° than that of uridine as shown in Fig. 2.10. Therefore, from Eq. (2.4), the intensity of NH2-uridine is weaker than that of uridine for the second peak of the CD spectra.

The experimental CD spectra of the uridine derivatives studied here are mainly of the intramolecular excitation nature within the nucleic-acid bases. Therefore, the

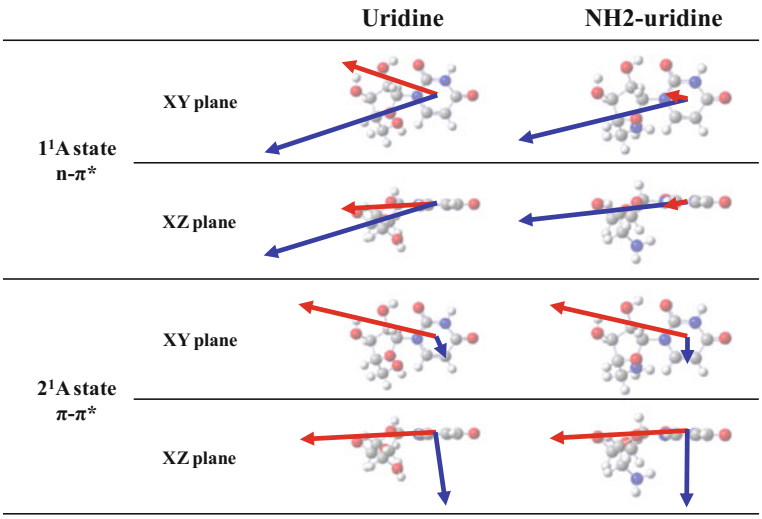

Fig. 2.10 Direction of ETDM (*red arrows*) and MTDM (*blue arrows*) of the 1 and 2^1A excited states of the anti-conformers of uridine and NH2-uridine. The unit of arrows of the 2^1A states is 2.5 times larger than that of the 1^1A states. Uracil is on the XY plane (Reprinted from Ref. [42] with permission from *The Journal of Physical Chemistry A* **2014**, *118*, 2931–2941. Copyright 2014 American Chemical Society.)

excited states of NH2-uridine are almost the same as those of uridine. However, the change of OH to NH2 leads to the difference of the dihedral angle of the optimized geometry, which weakens the intensity of the CD spectra. The differences are due to the magnitude of the ETDM for the first peak and due to the angle θ for the second peak.

2.6 Conformational Dependence of the CD Spectra of Deoxyguanosine

Deoxyguanosine (dG) is an important nucleic-acid base that composes DNA. The single bond between guanine and deoxyribose in dG can rotate almost freely: the energy barrier for the rotation is very low. Nevertheless, the CD spectrum is very sensitive to this rotational angle. In this section, we study the conformational dependence of the UV and CD spectra of dG. The SAC-CI spectra are given in red lines, and the experimental spectra measured in water solution are shown in black lines.

First, we studied the potential curve for the rotation around this single bond. Figure 2.11 shows the calculated potential curve for the rotation around this single bond by using the DFT method with B3LYP/6-31G(d,p). Other geometrical parameters were optimized at each rotational angle φ. The anti-dG was calculated to be more stable than the syn-dG by 0.47 kcal/mol, a very small difference. Since the energy barriers between the syn- and anti-dG are only 3–6 kcal/mol, the dG can rotate easily between the syn- and anti-conformations.

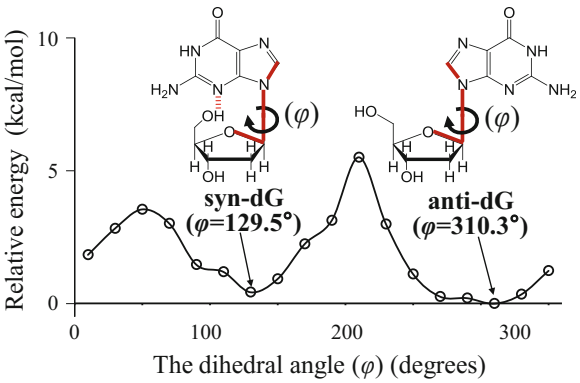

Fig. 2.11 Potential energy curve of the ground state of dG determined as dihedral angle φ is varied in increments of 20°. Other geometrical parameters were optimized at each φ (Reprinted from Ref. [40] with permission from *The Journal of Physical Chemistry A* **2013**, *117*, 42–55. Copyright 2013 American Chemical Society.)

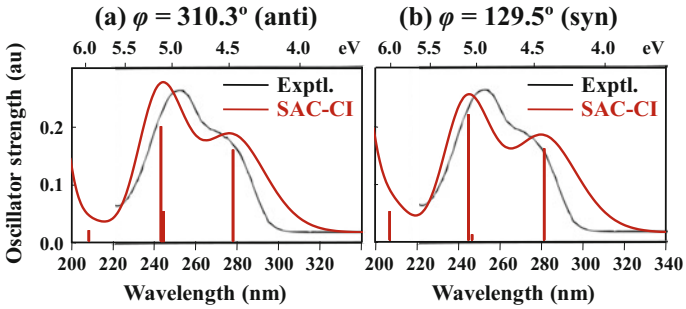

Fig. 2.12 SAC-CI UV spectra of **a** anti- and **b** syn-dG (*red*), compared with the experimentally determined UV spectrum of dG (*black* [52]) (Reprinted from Ref. [40] with permission from *The Journal of Physical Chemistry A* **2013**, *117*, 42–55. Copyright 2013 American Chemical Society.)

We first examined the UV spectra of the syn- and anti-conformers. Figure 2.12 shows the SAC-CI UV spectra (red line) of both anti- and syn-dG compared with the experimental (black) UV spectrum of dG. The SAC-CI UV spectra of both anti- and syn-dG are similar to the experimental UV spectrum. Therefore, it is difficult to determine whether the experimental UV spectrum of dG is due to the anti or the syn conformation.

Next, we calculated the CD spectra during the rotation around the syn- and anti-conformers. Figure 2.13 shows the SAC-CI CD spectra of dG at several dihedral angles φ between deoxyribose and guanine. For the experimental CD spectrum of dG (black line), the first band at 276 nm is very weak, the second band at 250 nm is strong negative, and the third band at 214 nm is strong positive. The experimental CD spectrum is in good agreement with the SAC-CI CD spectra of the anti-dG (φ = 310.3°) and the dG with φ = 330° (red lines of Fig. 2.13p and q). The Boltzmann averaged SAC-CI CD spectrum shown by the green line in Fig. 2.13s is also close to the experimental spectrum. However, the other SAC-CI CD spectra shown by red lines are different from the black experimental CD spectrum. Therefore, we concluded that the dG exists as an anti-conformation in water solution based on the comparisons with the experimental and SAC-CI CD spectra. Note that the same conclusion is also drawn from the theoretical potential energy curve of Fig. 2.11, if we can neglect the solute–solvent interactions.

Thus, the CD spectra largely depend on the rotation around the single bond though it is a very low-energy process. We can determine the conformation of the molecule in solution by comparing the SAC-CI CD spectra with the experimental CD spectrum.

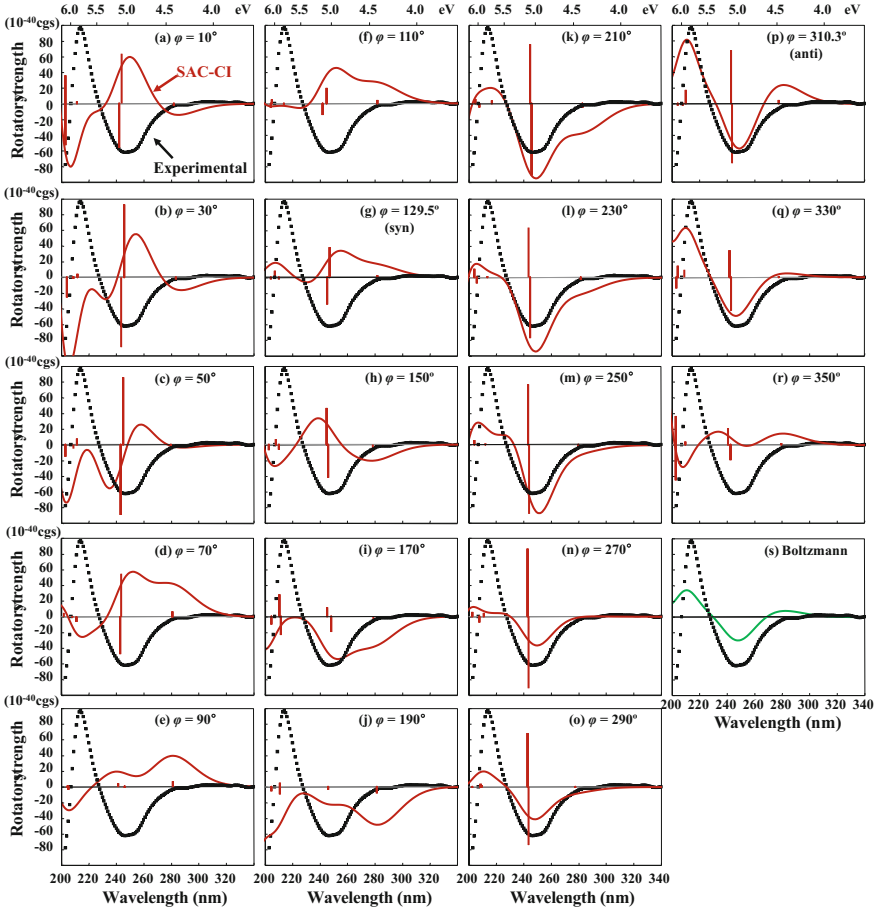

Fig. 2.13 CD spectra of dG at several conformation angles φ. The experimental CD spectrum [52] (*black line*) of dG is compared with the SAC–CI CD spectra (*red lines*) of **a** $\varphi = 10°$, **b** $\varphi = 30°$, **c** $\varphi = 50°$, **d** $\varphi = 70°$, **e** $\varphi = 90°$, **f** $\varphi = 110°$, **g** $\varphi = 129.5°$ (syn), **h** $\varphi = 150°$, **i** $\varphi = 170°$, **j** $\varphi = 190°$, **k** $\varphi = 210°$, **l** $\varphi = 230°$, **m** $\varphi = 250°$, **n** $\varphi = 270°$, **o** $\varphi = 290°$, **p** $\varphi = 310.3°$ (anti), **q** $\varphi = 330°$ and **r** $\varphi = 350°$. The Boltzmann averaged SAC–CI CD spectrum (*green line*, (s)) of all conformers is also shown (Reprinted from Ref. [40] with permission from *The Journal of Physical Chemistry A* **2013**, *117*, 42–55. Copyright 2013 American Chemical Society.)

2.7 Double-Helical Structure of DNA and the Nature of Weak Interactions Involved

A well-known B-DNA has a right-handed double-helical structure, while Z-DNA has a left-handed double-helical structure. When DNA has a special sequence, the transition from B- to Z-DNA or from Z- to B-DNA is induced by the changes in salt concentration or temperature [53–58]. The left-handed Z-DNA is preferred at low temperature or at high salt concentration, but the right-handed B-DNA is preferred at the reverse conditions [53–58]. The CD spectrum of Z-DNA is much different from that of B-DNA, while the UV spectra between B- and Z-DNA are similar [54–58]. The main difference lies in the sign at around 295 nm of the CD spectra. It is positive for B-DNA but negative for Z-DNA. Therefore, the CD spectroscopy can be used to identify the helical structure of DNA or RNA in solution. However, only a few theoretical studies have investigated why the sign of the CD spectrum of DNA changes by the type of its helical structure. We studied the SAC-CI CD spectra of DNA to elucidate the origin of the negative peak at around 295 nm of the CD spectrum of Z-DNA [40].

We considered three factors to be important that affect the CD spectra of DNA. They are the conformation of monomer, the hydrogen-bonding interactions, and the stacking interactions between the nucleic-acid bases. Figure 2.14 shows the computational models taken from the X-ray crystallographic structures of the B- and Z-DNA, in which deoxyguanosine (dG) and deoxycytidine (dC) are arranged alternately. Their existence ratio is unity. We calculated the monomer, dimer, and tetramer models. The effect of the conformation of dG and dC was verified by the monomer model. The hydrogen-bonding and stacking interactions were verified by the dimer and tetramer models. The dimer models include either the hydrogen-bonding or stacking interactions, but the tetramer models include both the hydrogen-bonding and stacking interactions.

2.7.1 Monomer Model

The dC has the anti-conformation in both B- and Z-DNA. However, the dG has the anti-conformation in B-DNA but syn conformation in Z-DNA. We compare the SAC-CI CD spectra of the anti- and syn-dG shown in Fig. 2.13 with the experimental CD spectra of B- and Z-DNA shown in Fig. 2.15 that was reported by Tran-Dinh et al. [54]. There, we notice that, in the second band region (near 250 nm), the SAC-CI CD spectra of anti- and syn-dG are similar to the experimental CD spectra of B- and Z-DNA, respectively.

Based on this observation, we considered the monomer model in which we examine whether the CD spectra of B- and Z-DNA could be understood from the CD spectra of monomers taking the geometries found in the B- and Z-DNA. Therefore, we calculated the SAC-CI CD spectra of the dG and dC monomers using

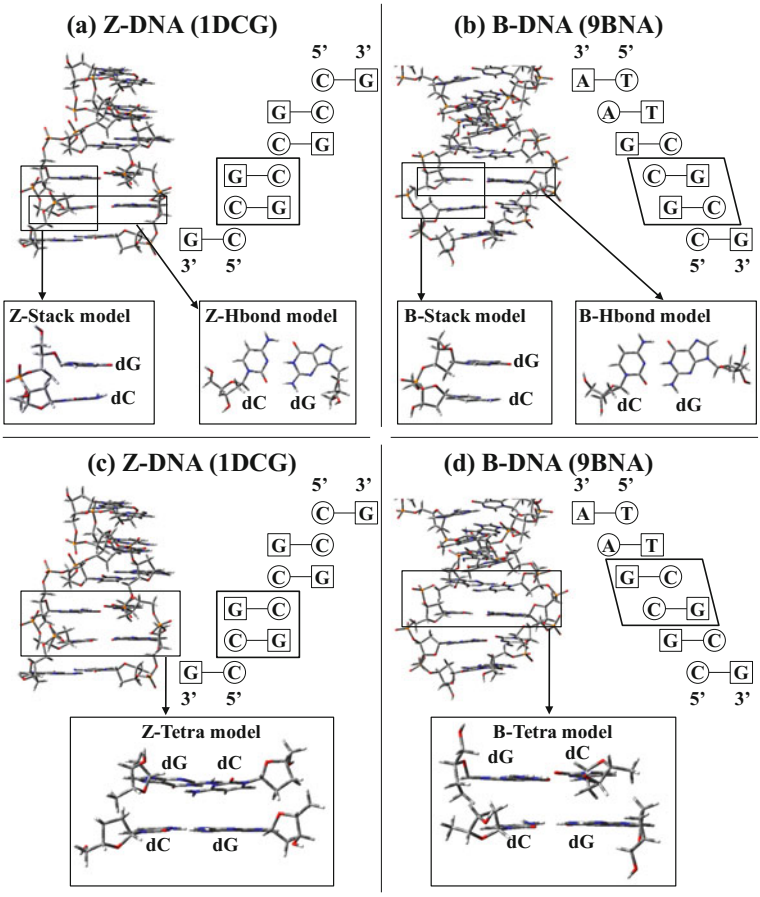

Fig. 2.14 Computational models. **a** Hydrogen-bonding (Z-Hbond) and stacking (Z-Stack) models taken from the X-ray crystallography structure (1DCG) of Z-DNA. **b** Hydrogen-bonding (B-Hbond) and stacking (B-Stack) models taken from the X-ray crystallography structure (9BNA) of B-DNA. **c** Tetramer (Z-Tetra) model taken from the X-ray crystallography structure (1DCG) of Z-DNA. **d** Tetramer (B-Tetra) model taken from the X-ray crystallography structure (9BNA) of B-DNA (Reprinted from Ref. [40] with permission from *The Journal of Physical Chemistry A* **2013**, *117*, 42–55. Copyright 2013 American Chemical Society.)

their geometries in the X-ray crystallographic structures of the B- and Z-DNA and the results were summarized in Fig. 2.15. In this figure, the composite CD spectra are the sums of the SAC-CI CD spectra of dG and dC in Z-DNA and B-DNA.

Very roughly speaking, for B-DNA, the composite SAC-CI CD spectrum shown in a magenta color is similar to the experimental CD spectrum shown in a black color. However, for Z-DNA, the SAC-CI composite spectrum in a magenta color does not explain a large negative peak near 290 nm of the experimental spectrum

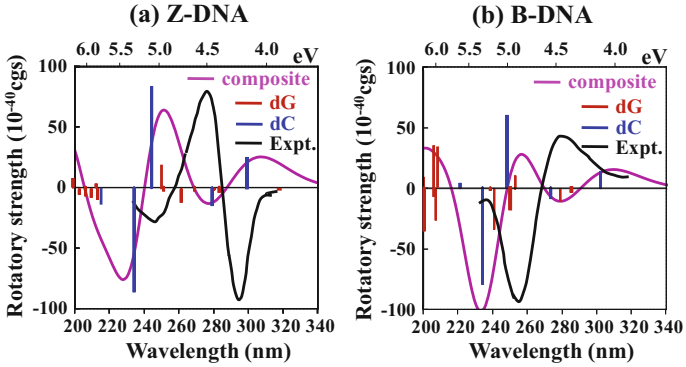

Fig. 2.15 SAC-CI CD spectra of the composite CD spectra of **a** Z-DNA and **b** B-DNA obtained from the SAC-CI CD spectra of dG and dC, compared with the experimental CD spectra [54] (*black lines*) of Z-DNA and B-DNA. The *red* and *blue lines* represent the excited state of dG and dC, respectively. The magenta line represents the composite spectra that are the sum of the CD spectra of dG and dC (Reprinted from Ref. [40] with permission from *The Journal of Physical Chemistry A* **2013**, *117*, 42–55. Copyright 2013 American Chemical Society.)

shown in a black color. Therefore, we must say that the monomer model alone is insufficient to explain the difference in the experimental CD spectra between B- and Z-DNA. More refined models are necessary, and we explain them below.

2.7.2 Dimer Model

We now calculate the SAC-CI CD spectra with the dimer models that include either the hydrogen-bonding interaction or the stacking interaction between dG and dC as shown in Fig. 2.14a and b, respectively. Most importantly, the monomer model could not account for the negative peak at 295 nm. Figure 2.16 shows the SAC-CI CD spectra obtained with the dimer models, compared with the experimental CD spectra of B- and Z-DNA. In the experimental CD spectrum given with the black line, the first peak is negative at 296 nm and the second peak is positive at 275 nm for Z-DNA, while the first peak is positive at 280 nm and the second peak is negative at 255 nm for B-DNA. On the other hand, among the four SAC-CI CD spectra, the sign at 295 nm is negative with only the Z-Stack model. Since the dG strongly stacks with the dC in only the Z-Stack model as shown in Fig. 2.14a, the stacking interaction between dG and dC can account for the strong negative peak at 295 nm of the CD spectra in Z-DNA. This CD peak is due to the 1^1A excited state from the HOMO to the LUMO in dC. The stacking interaction with dG changes the sign of the rotatory strength of the 1^1A excited state from the positive of the monomer model to the negative of the Z-stack model. However, since the stacking interaction of B-DNA is weaker than that of Z-DNA as shown in Fig. 2.14b, such

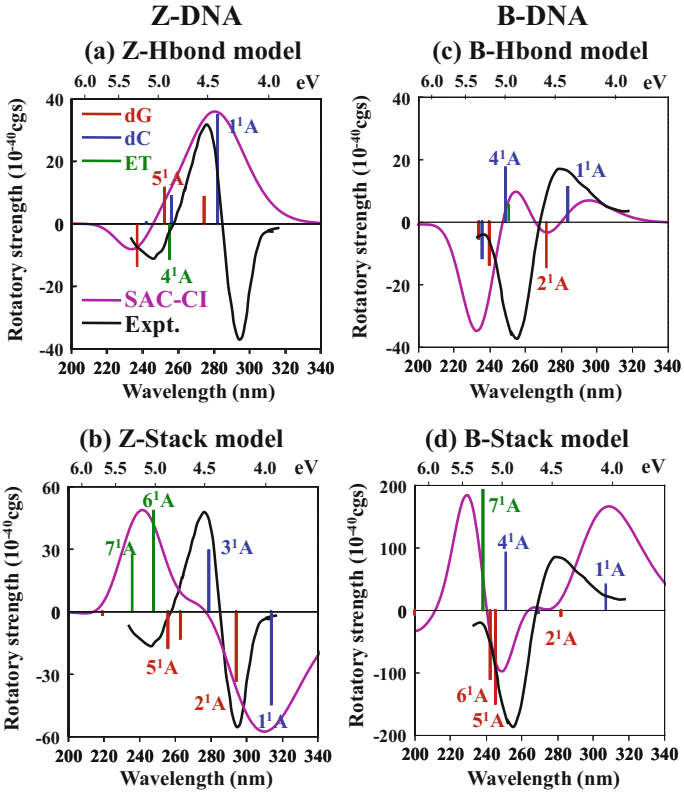

Fig. 2.16 SAC-CI CD spectra for the dimer models. The SAC-CI spectra (*magenta line*) of **a** Z-Hbond model, **b** Z-Stack model, **c** B-Hbond model and **d** B-Stack model are compared with the experimental CD spectra [54] (*black line*) of Z-DNA (**a**, **b**) and B-DNA (**c**, **d**). The *red* and *blue lines* represent the intramolecular excited states of dG and dC, respectively. The *green lines* represent the electron transfer (ET) excited state from dG to dC (Reprinted from Ref. [40] with permission from *The Journal of Physical Chemistry A* **2013**, *117*, 42–55. Copyright 2013 American Chemical Society.)

change in the sign does not occur near 295 nm so that the negative peak does not appear at around 295 nm for the B-Stack model. Therefore, we can conclude that the negative peak at 295 nm is originated from the stacking interaction between the nucleic-acid bases.

In the hydrogen-bonding models (Z-Hbond and B-Hbond), the excitation energy of the first excited state was calculated to be at a higher energy region than those of the monomer models and the stacking dimer models. However, the rotatory strength is positive for both hydrogen-bonding models. Therefore, we concluded that the

hydrogen-bonding interaction affects the excitation energies of the lowest excited states but are not the origin of the negative peak at around 295 nm of the CD spectra.

2.7.3 Tetramer Model

Finally, we calculated the SAC-CI CD spectra with the tetramer models that include both of the hydrogen-bonding and stacking interactions. Figure 2.17 shows the

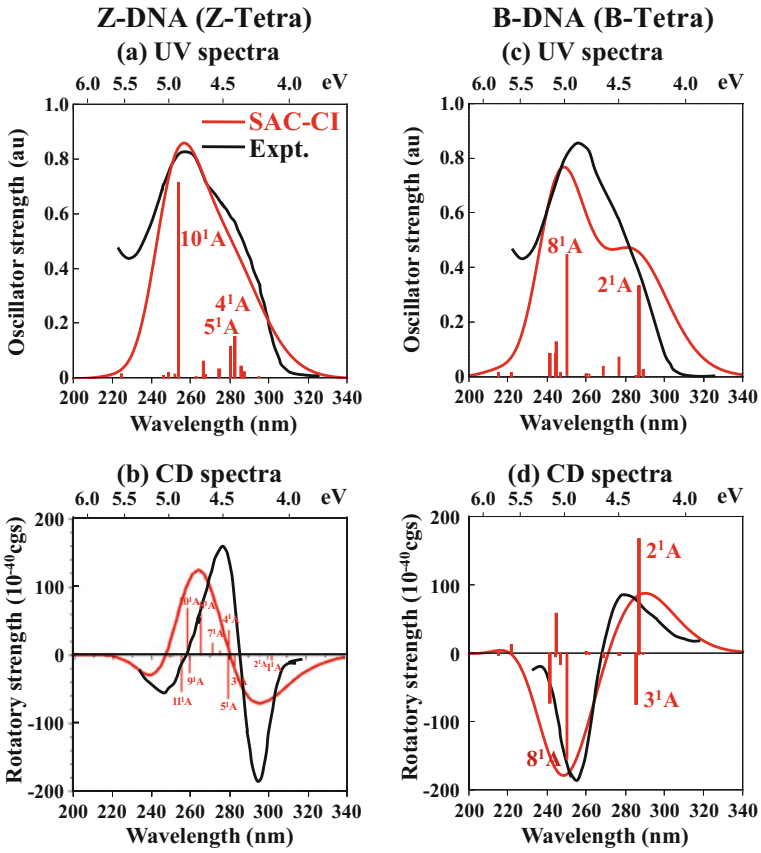

Fig. 2.17 SAC-CI UV and CD spectra for the tetramer models. The SAC-CI spectra (*red line*) of Z-Tetra model (**a**, **b**) and B-Tetra model (**c**, **d**) compared with the experimental UV and CD spectra [54] (*black line*) of Z-DNA (**a**, **b**) and B-DNA (**c**, **d**). All excited states of SAC-CI calculations have been shifted to the lower values by 0.5 eV (Refs. [40, 43]). (Reprinted from Refs. [40] and [43] with permission from *The Journal of Physical Chemistry A* **2013**, *117*, 42–55, **2015**, *119*, 8269–8278. Copyright 2013, 2015 American Chemical Society.)

SAC-CI UV and CD spectra of the tetramer models compared with the experimental UV and CD spectra of the B- and Z-DNA. The SAC-CI UV spectrum of the Z-Tetra model reproduced the main and shoulder peaks of the experimental UV spectrum of Z-DNA. However, for the B-Tetra model, the shoulder peak is slightly different from the experiment, because the angle between the two bases in the hydrogen-bonding base pair is larger for the B-Tetra model than that of the Z-Tetra model [44].

The SAC-CI CD spectrum of the B-Tetra model was in good agreement with the experimental CD spectrum of B-DNA for the sign as well as the intensity. The SAC-CI CD spectrum of the Z-Tetra model also reproduced the general features of the experimental CD spectrum of Z-DNA.

The lowest excited state of the Z-Tetra model is the electron-transfer (ET) excited state from dG to dC through the stacking conformation, but for the B-Tetra model it is the intramolecular excitation within dC. Thus, the ET excited state is the origin of the strong negative peak at 295 nm of Z-DNA. We concluded that the hydrogen-bonding interaction changes the excitation energy of the lowest excited state and that the stacking interaction is the origin of the negative peak at 295 nm of the CD spectra.

2.8 CD Spectra Is an Indicator of the Stacking Interaction in Double-Helical DNA

As noted in the above section, the negative peak at 295 nm is caused by the stacking interaction between the two base pairs of dG and dC. To verify the relationship between the stacking interaction and the intensity of the peak at 295 nm of the CD spectra of DNA, we calculated the SAC-CI CD spectra for the different distances using the tetramer model of Z-DNA as shown in Fig. 2.18.

Figure 2.19 shows the SAC-CI CD spectra for the different distance R between the two base pairs using the tetramer models of Z-DNA. The experimental CD spectra of the Z- and B-DNA are shown with the solid and dotted black lines, respectively. The negative peak at 295 nm has the strongest intensity for $\Delta R = 0.0$ Å (X-ray crystallographic structure). The intensity of the negative peak at 295 nm becomes weaker and weaker as the distance between the two base pairs (ΔR) increases. Note that the intensity at 295 nm is weaker for $\Delta R = -0.2$ Å than for $\Delta R = \pm 0.0$ Å.

In addition, as the distance ΔR increases, the SAC-CI CD spectra come close to the experimental CD spectrum of B-DNA (dotted black line) from that of the Z-DNA (solid black line). Although the conformations of dG and dC are much

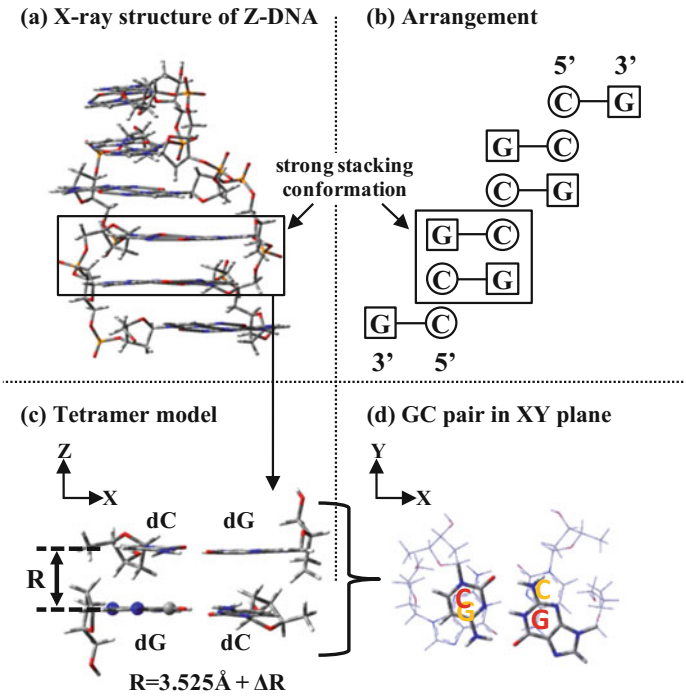

Fig. 2.18 **a** X-ray crystallography structure of Z-DNA (PDB ID: 1DCG). **b** Arrangement of cytosine (C) and guanine (G). **c** Geometry of tetramer model. R represents the distance between the two base pairs. R is 3.525 Å from the X-ray crystallography structure. **d** Geometry of two GC (dG and dC) pairs. Three atoms indicated by "Ball" are arranged on the XY plane (Reprinted from Ref. [43] with permission from *The Journal of Physical Chemistry A* **2015**, *119*, 8269–8278. Copyright 2013 American Chemical Society.)

different from the structure of B-DNA, the SAC-CI CD spectrum of the $\Delta R = +2.0$ Å model is in good agreement with the experimental CD spectrum of B-DNA due to the weak stacking interaction.

The negative peak at 295 nm is caused by the electron-transfer (ET) excited state from dG to dC through the stacking interaction at around $\Delta R = \pm 0.0$ Å, but when the distance between dG and dC increases, the excitations at around 295 nm become intra dG and dC excitations for around $\Delta R = +2.0$ Å. The ET excited state is calculated to be at higher energy region for $\Delta R = +2.0$ Å. Since the two base pairs strongly stack for Z-DNA but weakly stack for B-DNA, the negative peak at 295 nm becomes the indicator of the stacking interaction between the two base pairs.

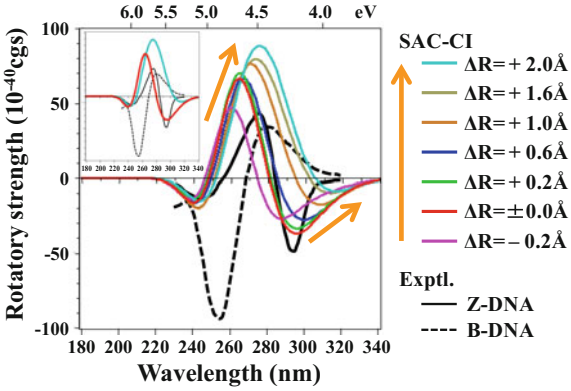

Fig. 2.19 SAC-CI CD spectra (*colored lines*) for the different distance R between the two base pairs using the tetramer models of Z-DNA compared with the experimental CD spectra of Z- and B-DNA (*black lines*) [54]. All excited states of the SAC-CI calculation have been shifted to the lower values by 0.5 eV. The *magenta*, *red*, *green*, *blue*, *gold*, *khaki* and *cyan lines* represent the SAC-CI CD spectra with $\Delta R = -0.2, \pm 0.0, +0.2, +0.6, +1.0, +1.6$ and $+2.0$ Å. The black solid and dotted lines represent the experimental CD spectra of Z- and B-DNA, respectively. The orange arrows represent the direction of the SAC-CI CD spectral change in the increase of the distance R. The *inset* shows the two representative SAC-CI spectra with $\Delta R = \pm 0.0$ Å and $\Delta R = +2.0$ Å compared with the experimental CD spectra of Z-and B-DNA (Reprinted from Ref. [43] with permission from *The Journal of Physical Chemistry A* **2015**, *119*, 8269–8278. Copyright 2013 American Chemical Society.)

2.9 Similarities and Differences Between Double-Helical DNA and RNA

RNA (ribonucleic acid) can also form both the right- and left-handed double-helical structures. The transition between the right-handed A-RNA and the left-handed Z-RNA can be induced by the changes by salt concentration or temperature [59–61]. These phenomena are quite similar to those of DNA. However, the feature of the CD spectra of RNA is quite different from that of DNA. For the CD spectra of the right-handed A-RNA, the first band at 295 nm has a negative sign and the second band has a positive sign [59–61], which is similar to the feature of the left-handed Z-DNA. On the other hand, the features of the CD spectra of the left-handed Z-RNA are similar to those of the right-handed B-DNA. In addition, the right-handed A-RNA is preferred at low temperature [59–61], similarly to the left-handed Z-DNA. Namely, the features of the CD spectra of RNA are opposite to those of DNA.

We calculated the SAC-CI CD spectra of DNA and RNA to clarify the relationship between the helical structures and their CD spectra, and to elucidate the similarities and differences between DNA and RNA. The geometries were taken from the X-ray crystallographic structures and shown in Fig. 2.20. These structures are composed of 12 nucleic-acid bases and have the same sequence in which dG

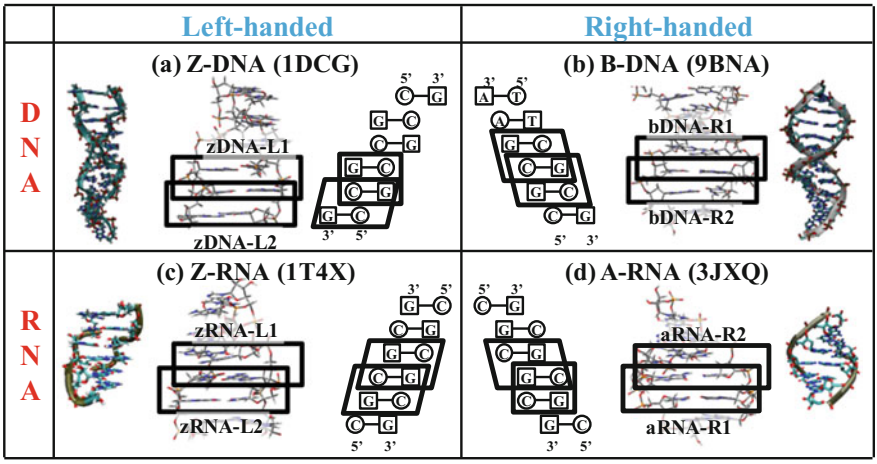

Fig. 2.20 Tetramer models (zDNA-L1, zDNA-L2, bDNA-R1, bDNA-R2, zRNA-L1, zRNA-L2, aRNA-R1 and aRNA-R2) taken from the X-ray crystallographic structures of **a** Z-DNA (1DCG), **b** B-DNA (9BNA), **c** Z-RNA (1T4X) and **d** A-RNA (3JXQ). "G" and "C" represent guanine and cytosine, respectively (Reprinted from Ref. [44] with permission from *The Journal of Physical Chemistry A* **2016**, *120*, 9008–9018. Copyright 2016 American Chemical Society.)

and dC for DNA and guanosine (G) and cytidine (C) for RNA are arranged alternately. We calculated the CD spectra of two tetramer models for each DNA and RNA, because each DNA or RNA includes two kinds of the stacking interactions as seen from Fig. 2.20.

We show in Fig. 2.21 the SAC-CI CD spectra of the tetramer models of Z-DNA, B-DNA, Z-RNA and A-RNA, compared with their experimental CD spectra measured in water solution [58, 61]. The SAC-CI CD spectra seemed to be not in good agreement with the experimental CD spectra at first glance. However, the SAC-CI CD spectra of the zDNA-L1 and aRNA-R1 models were in good correspondence with the experimental CD spectra of Z-DNA and A-RNA, respectively. The negative peak at 295 nm corresponds to the lowest two excited states that are the electron transfer (ET) excitations from guanine to cytosine through the stacking interaction. But the SAC-CI CD spectra of the zDNA-L2 and aRNA-R2 models were opposite to those of the zDNA-L1 and aRNA-R1 models. Even though we used the tetramer models taken from the same helical structures, the negative peak did not appear at 295 nm in the CD spectra due to the weak stacking interaction (Fig. 2.20a, d). Namely, the negative peak observed at 295 nm is due to the ET excitation from guanine to cytosine through the strong stacking interaction in both DNA and RNA: The peak at 295 nm can be considered to be the indicator of the strong stacking interaction for the double-helical structures of DNA as well as RNA.

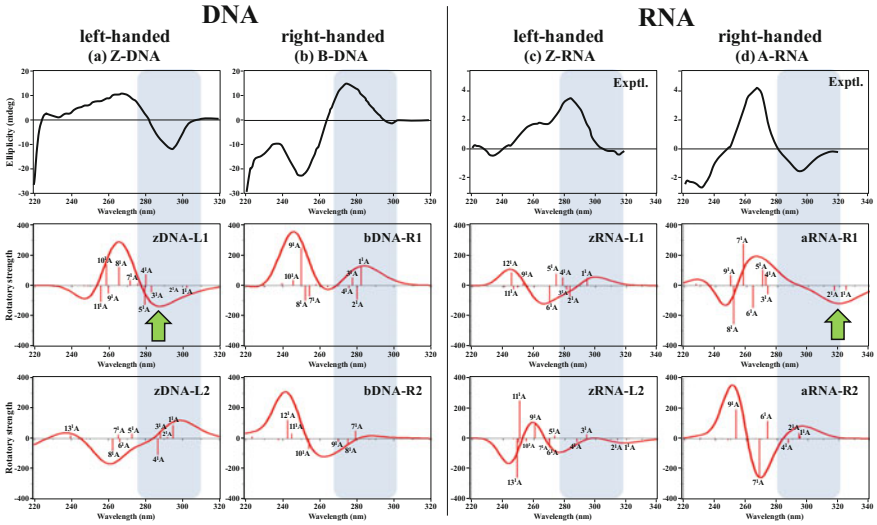

Fig. 2.21 SAC-CI CD spectra (*red lines*) of the eight tetramer models compared with the experimental CD spectra (*black lines*) [58, 61]. All excited states of SAC-CI calculations have been shifted to the lower sides by the values of 0.5 eV for DNA and 0.7 eV for RNA, respectively. *Blue-colored squares* represent the first band region of the CD spectra of each DNA or RNA. The negative peaks at 295 nm are shown by *green arrows* (Reprinted from Ref. [44] with permission from *The Journal of Physical Chemistry A* **2016**, *120*, 9008–9018. Copyright 2016 American Chemical Society.)

2.10 Conclusion

The ChiraSac method is a useful tool for analyzing and clarifying the chemical information included in the CD spectra of chiral molecules and molecular systems. The CD spectra depend strongly on the conformational changes due to the rotations around the single bonds. Since this rotation is a low-energy process, it may reflect the natures of the low-energy molecular interactions with solvents and with the molecular environments. With HPAA (α-hydroxyphenylacetic acid) and dG (Deoxyguanosine), we have shown that the calculations of the CD spectra with a reliable theory like SAC-CI are useful to clarify the rotational conformation of a molecule in solution, which may be different from the stable conformation in a gas phase. Since the calculated CD spectrum is the result of the cancellations of many different peaks of positive and negative intensities, the theory must be reliable enough in both peak positions and intensities (rotatory strengths). Generally speaking, the TD-DFT calculations are not reliable enough in the qualities of these quantities, and therefore, detailed analyzes and understanding are difficult with the TD-DFT calculations. The present overview of the results of the SAC-CI calculations of the CD spectra of molecules and molecular systems supports the reliability of the SAC-CI theory. The ChiraSac method is a theoretical methodology of

investigating the chemistry and physics of chiral molecules and molecular systems using the Gaussian suite of programs involving the SAC-CI method and other many useful methods. Actually, in the studies of DNA and RNA, for example, we used many features of the SAC-CI and DFT methods in systematized ways involved in Gaussian. The ChiraSac studies could elucidate the information of the low-energy processes and the nature of the weak interactions involved in the observed CD spectra by using a highly reliable excited-state theory, the SAC-CI method, together with the many efficient methodologies involved in Gaussian. With the ChiraSac method, one can study many different subjects related to chirality, such as the conformations of chiral molecules in solutions or proteins, the low-energy processes such as the rotations around the single bonds of chiral atoms and the natures of the weak interactions such as the hydrogen-bonding and stacking interactions, van der Waals forces, solvent effects, etc. Therefore, the ChiraSac method will become a useful molecular technology for the material and drug designs.

Acknowledgements The computations were carried out using the computers at the Research Center for Computational Science, Okazaki, Japan, whom we acknowledge sincerely. We also thank the support of Mr. Nobuo Kawakami for the researches of QCRI. This work was supported by JSPS KAKENHI, Grant Numbers 15K05408 and 16H02257.

References

1. H. Nakatsuji, K. Hirao, Cluster expansion of the wavefunction. Symmetry-adapted-cluster expansion, its variational determination, and extension of open-shell orbital theory. J. Chem. Phys. **68**, 2053–2065 (1978)
2. H. Nakatsuji, Cluster expansion of the wavefunction. Excited states. Chem. Phys. Lett. **59**, 362–364 (1978)
3. H. Nakatsuji, Cluster expansion of the wavefunction. Electron correlations in ground and excited states by SAC (Symmetry-Adapted-Cluster) and SAC-CI theories. Chem. Phys. Lett. **67**, 329–333 (1979)
4. H. Nakatsuji, Cluster expansion of the wavefunction. Calculation of electron correlations in ground and excited states by SAC and SAC-CI theories. Chem. Phys. Lett. **67**, 334–342 (1979)
5. H. Nakatsuji, Description of two- and many-electron processes by the SAC-CI method. Chem. Phys. Lett. **177**, 331–337 (1991)
6. H. Nakatsuji, M. Ehara, Symmetry-adapted cluster-configuration interaction method applied to high-spin multiplicity. J. Chem. Phys. **98**, 7179–7184 (1993)
7. T. Nakajima, H. Nakatsuji, Analytical energy gradient of the ground, excited, ionized and electron-attached states calculated by the SAC/SAC-CI method. Chem. Phys. Lett. **280**, 79–84 (1997)
8. T. Nakajima, H. Nakatsuji, Energy gradient method for the ground, excited, ionized, and electron-attached states calculated by the SAC (symmetry-adapted cluster)/SAC-CI (configuration interaction) method. Chem. Phys. **242**, 177–193 (1999)
9. M. Ishida, K. Toyota, M. Ehara, H. Nakatsuji, Analytical energy gradients of the excited, ionized and electron-attached states calculated by the SAC-CI general-R method. Chem. Phys. Lett. **347**, 493–498 (2001)
10. M. Ishida, K. Toyota, M. Ehara, H. Nakatsuji, Analytical energy gradient of high-spin multiplet state calculated by the SAC-CI method. Chem. Phys. Lett. **350**, 351–358 (2001)

11. K. Toyota, M. Ehara, H. Nakatsuji, Elimination of singularities in molecular orbital derivatives: Minimum Orbital-Deformation (MOD) method. Chem. Phys. Lett. **356**, 1–6 (2002)
12. K. Toyota, M. Ishida, M. Ehara, M.J. Frisch, H. Nakatsuji, Singularity-free analytical energy gradients for the SAC/SAC-CI method: Coupled Perturbed Minimum Orbital-Deformation (CPMOD) approach. Chem. Phys. Lett. **367**, 730–736 (2003)
13. M. Ishida, K. Toyota, M. Ehara, M.J. Frisch, H. Nakatsuji, Analytical energy gradient of the symmetry-adapted-cluster configuration-interaction general-R method for singlet to septet ground and excited states. J. Chem. Phys. **120**, 2593–2605 (2004)
14. Gaussian 09, Revision E.01, M.J. Frisch, G.W. Trucks, H.B. Schlegel, G.E. Scuseria, M.A. Robb, J.R. Cheeseman, G. Scalmani, V. Barone, B. Mennucci, G.A. Petersson, H. Nakatsuji, M. Caricato, X. Li, H.P. Hratchian, A.F. Izmaylov, J. Bloino, G. Zheng, J.L. Sonnenberg, M. Hada, M. Ehara, K. Toyota, R. Fukuda, J. Hasegawa, M. Ishida, T. Nakajima, Y. Honda, O. Kitao, H. Nakai, T. Vreven, J.A. Montgomery Jr., J.E. Peralta, F. Ogliaro, M. Bearpark, J. J. Heyd, E. Brothers, K.N. Kudin, V.N. Staroverov, R. Kobayashi, J. Normand, K. Raghavachari, A. Rendell, J.C. Burant, S.S. Iyengar, J. Tomasi, M. Cossi, N. Rega, J.M. Millam, M. Klene, J.E. Knox, J.B. Cross, V. Bakken, C. Adamo, J. Jaramillo, R. Gomperts, R. E. Stratmann, O. Yazyev, A.J. Austin, R. Cammi, C. Pomelli, J.W. Ochterski, R.L. Martin, K. Morokuma, V.G. Zakrzewski, G.A. Voth, P. Salvador, J.J. Dannenberg, S. Dapprich, A.D. Daniels, Ö. Farkas, J.B. Foresman, J.V. Ortiz, J. Cioslowski, D.J. Fox, Gaussian, Inc., Wallingford, CT, 2009.
15. H. Nakatsuji, Electronic structures of ground, excited, ionized, and anion states studied by the SAC/SAC-CI theory. Acta Chim. Hung. Models Chem. **129**, 719–776 (1992)
16. H. Nakatsuji, SAC-CI Method: theoretical aspects and some recent topics, in *Computational Chemistry—Reviews of Current Trends*, ed. by J. Leszczynski, vol. 2 (World Scientific, Singapore, 1997), pp. 62–124
17. M. Ehara, M. Ishida, K. Toyota, H. Nakatsuji, SAC-CI general-R Method: theory and applications to the multi-electron processes, in *Reviews of Modern Quantum Chemistry (A Celebration of the Contributions of Robert G. Parr)*, ed. by K.D. Sen (World Scientific, Singapore, 2003), pp. 293–319
18. H. Nakatsuji, Deepening and extending the quantum principles in chemistry. Bull. Chem. Soc. Jpn. **78**, 1705–1724 (2005)
19. M. Ehara, J. Hasegawa, H. Nakatsuji, SAC-CI method applied to molecular spectroscopy, in *Theory and Applications of Computational Chemistry: The First Forty Years,* ed. by C.E. Dykstra, G. Frenking, K.S. Kim, G.E. Scuseria (Elsevier, Oxford, U.K., 2005), pp. 1099–1141
20. J. Hasegawa, H. Nakatsuji, Exploring photo-biology and bio-spectroscopy with the SAC-CI (Symmetry-Adapted Cluster-Configuration Interaction) method, in *Radiation Induced Molecular Phenomena in Nucleic Acid: A Comprehensive Theoretical and Experimental Analysis*, ed. by M. Shukla, J. Leszczynsk (Springer, 2008), Chapter 4, pp. 93–124
21. N. Berova, K. Nakanishi, R.W. Woody (eds.), *Circular Dichroism: Principles and Applications* (Wiley-VCH, New York, 2000)
22. N. Berova, P.L. Polavarapu, K. Nakanishi, R.W. Woody (eds.), *Comprehensive Chiroptical Spectroscopy: Applications in Stereochemical Analysis of Synthetic Compounds, Natural Products, and Biomolecules,* vol. 2 (Wiley, Hoboken, New Jersey, 2012)
23. C. Niederalt, S. Grimme, S.D. Peyerimhoff, A. Sobanski, F. Vögtle, M. Lutz, A.L. Spek, M. J. van Eis, W.H. de Wolf, F. Bickelhaupt, Chiroptical properties of 12,15-dichloro[3.0] orthometacyclophane—correlations between molecular structure and circular dichroism spectra of a biphenylophane. Tetrahedron: Asymmetry **10**, 2153–2164 (1999)
24. F. Vögtle, S. Grimme, J. Hormes, K.H. Dötz, N. Krause, Theoretical simulations of electronic circular dichroism spectra, in *Interactions in Molecules: Electronic and Steric Effects*, ed. by S.D. Peyerimhoff (Wiley-VCH, Weinheim, 2003), pp. 66–109

25. F.E. Jorge, J. Autschbach, T. Ziegler, On the origin of optical activity in tris-diamine complexes of Co(III) and Rh(III): a simple model based on time-dependent density function theory. J. Am. Chem. Soc. **127**, 975–985 (2005)
26. H. Komori, Y. Inai, Electronic CD study of a helical peptide incorporating Z-dehydrophenylalanine residues: conformation dependence of the simulated CD spectra. J. Phys. Chem. A **110**, 9099–9107 (2006)
27. T.D. Crawford, M.C. Tam, M.L. Abrams, The current state of ab initio calculations of optical rotation and electronic circular dichroism spectra. J. Phys. Chem. A **111**, 12057–12068 (2007)
28. E. Botek, B. Champagne, Circular dichroism of helical structures using semiempirical methods. J. Chem. Phys. **127**, 204101-1–9 (2007)
29. E. Giorgio, K. Tanaka, L. Verotta, K. Nakanishi, N. Berova, C. Rosini, Determination of the absolute configurations of flexible molecules: Synthesis and theoretical simulation of electronic circular dichroism/optical rotation of some pyrrolo[2,3-b]indoline alkaloids—a case study. Chirality **19**, 434–445 (2007)
30. Y. Ding, X.C. Li, D. Ferreira, Theoretical calculation of electronic circular dichroism of the rotationally restricted 3,8''-biflavonoid morelloflavone. J. Org. Chem. **72**, 9010–9017 (2007)
31. G. Bringmann, T.A.M. Gulder, M. Reichert, T. Gulder, The online assignment of the absolute configuration of natural products: HPLC-CD in combination with quantum chemical CD calculations. Chirality **20**, 628–642 (2008)
32. T. Grkovic, Y. Ding, X.C. Li, V.L. Webb, D. Ferreira, B.R. Copp, Enantiomeric discorhabdin alkaloids and establishment of their absolute configurations using theoretical calculations of electronic circular dichroism spectra. J. Org. Chem. **73**, 9133–9136 (2008)
33. A. Shimizu, T. Mori, Y. Inoue, S. Yamada, Combined experimental and quantum chemical investigation of chiroptical properties of nicotinamide derivatives with and without intramolecular cation−π interactions. J. Phys. Chem. A **113**, 8754–8764 (2009)
34. J. Fan, T. Ziegler, A theoretical study on the exciton circular dichroism of propeller-like metal complexes of bipyridine and tripodal tris(2-pyridylmethyl)amine derivatives. Chirality **23**, 155–166 (2011)
35. J. Lambert, R.N. Compton, T.D. Crawford, The optical activity of carvone: a theoretical and experimental investigation. J. Chem. Phys. **136**, 114512-1–12 (2012)
36. S. Bureekaew, J. Hasegawa, H. Nakatsuji, Electronic circular dichroism spectrum of uridine studied by the SAC-CI method. Chem. Phys. Lett. **425**, 367–371 (2006)
37. Y. Honda, A. Kurihara, M. Hada, H. Nakatsuji, Excitation and circular dichroism spectra of (-)-(3aS,7aS)-2-chalcogena-trans-hydrindans (Ch=S, Se, Te): SAC and SAC-CI calculations. J. Comput. Chem. **29**, 612–621 (2008)
38. T. Miyahara, J. Hasegawa, H. Nakatsuji, Circular dichroism and absorption spectroscopy for three-membered ring compounds using Symmetry-Adapted Cluster-Configuration Interaction (SAC-CI) method. Bull. Chem. Soc. Jpn **82**, 1215–1226 (2009)
39. Y. Honda, A. Kurihara, Y. Kenmochi, M. Hada, Excitation and circular dichroism spectra of (+)-(S, S)-bis(2-methylbutyl)chalcogenides. Molecules **15**, 2357–2373 (2010)
40. T. Miyahara, H. Nakatsuji, H. Sugiyama, Helical structure and circular dichroism spectra of DNA: a theoretical study. J. Phys. Chem. A **117**, 42–55 (2013)
41. T. Miyahara, H. Nakatsuji, Conformational dependence of the circular dichroism spectrum of α-hydroxyphenylacetic acid: a ChiraSac study. J. Phys. Chem. A **117**, 14065–14074 (2013)
42. T. Miyahara, H. Nakatsuji, T. Wada, Circular dichroism spectra of uridine derivatives: ChiraSac study. J. Phys. Chem. A **118**, 2931–2941 (2014)
43. T. Miyahara, H. Nakatsuji, Indicator of the stacking interaction in the DNA double-helical structure: ChiraSac study. J. Phys. Chem. A **119**, 8269–8278 (2015)
44. T. Miyahara, H. Nakatsuji, H. Sugiyama, Similarities and differences between RNA and DNA double-helical structures in circular dichroism spectroscopy: a SAC-CI study. J. Phys. Chem. A **120**, 9008–9018 (2016)
45. L. Rosenfeld, Quantum-mechanical theory of the natural optical activity of liquids and gases. Z. Physik **52**, 161–174 (1929)

46. M. Pericou-Cayere, M. Rerat, A. Dargelos, Theoretical treatment of the electronic circular dichroism spectrum and the optical rotatory power of H_2S_2. Chem. Phys. **226**, 297–306 (1998)
47. W. Moffitt, Optical rotatory dispersion of helical polymers. J. Chem. Phys. **25**, 467–478 (1956)
48. A. Breest, P. Ochmann, F. Pulm, K.H. Gödderz, M. Carnell, J. Hormes, Experimental circular dichroism and VUV spectra of substituted oxiranes and thiiranes. Mol. Phys. **82**, 539–551 (1994)
49. L. Verbit, P.J. Heffron, Optically active aromatic chromophores-IV. Circular dichroism studies of some open-chain systems. Tetrahedron **24**, 1231–1236 (1968)
50. T. Wada, N. Minamimoto, Y. Inaki, Y. Inoue, Conformational and orientational switching of uridine derivatives by borates. Chem. Lett. **10**, 1025–1026 (1998)
51. D.W. Miles, R.K. Robins, H. Eyring, Optical rotatory dispersion, circular dichroism, and absorption studies on some naturally occurring ribonucleosides and related derivatives. Proc. Natl. Acad. Sci. U.S.A. **57**, 1138–1145 (1967)
52. H. Sugiyama, unpublished
53. A. Rich, A. Nordheim, A.H.-J. Wang, The chemistry and biology of left-handed Z-DNA. Ann. Rev. Biochem. **53**, 791–846 (1984)
54. S. Tran-Dinh, J. Taboury, J.-M. Neumann, T. Huynh-Dinh, B. Genissel, B. Langlois d'Estaintot, J. Igolen, ^{1}H NMR and circular dichroism studies of the B and Z conformations of the self-complementary deoxyhexanucleotide d(m^5C-G-C-G-m^5C-G): mechanism of the Z-B-coil transitions. Biochemistry **23**, 1362–1371 (1984)
55. H. Sugiyama, K. Kawai, A. Matsunaga, K. Fujimoto, I. Saito, H. Robinson, A.H.-J. Wang, Synthesis, structure and thermodynamic properties of 8-methylguanine-containing oligonucleotides: Z-DNA under physiological salt conditions. Nucl. Acid. Res. **24**, 1272–1278 (1996)
56. K. Kawai, I. Saito, H. Sugiyama, Conformation Dependent photochemistry of 5-halouracil-containing DNA: stereospecific 2'α-hydroxylation of deoxyribose in Z-form DNA. J. Am. Chem. Soc. **121**, 1391–1392 (1999)
57. T. Oyoshi, K. Kawai, H. Sugiyama, Efficient C2'α-hydroxylation of deoxyribose in protein-induced Z-form DNA. J. Am. Chem. Soc. **125**, 1526–1531 (2003)
58. Y. Xu, R. Ikeda, H. Sugiyama, 8-methylguanosine: a powerful Z-DNA stabilizer. J. Am. Chem. Soc. **125**, 13519–13524 (2003)
59. K. Hall, P. Cruz, I. Tinoco Jr., T.M. Jovin, J.H. van de Sande, 'Z-RNA'—a left-handed RNA double helix. Nature **311**, 584–586 (1984)
60. B.A. Brown II, K. Lowenhaupt, C.M. Wilbert, E.B. Hanlon, A. Rich, The Zα domain of the editing enzyme dsRNA adenosine deaminase binds left-handed Z-RNA as well as Z-DNA. Proc. Natl. Acad. Sci. U.S.A. **97**, 13532–13536 (2000)
61. R. Tashiro, H. Sugiyama, biomolecule-based switching devices that respond inversely to thermal stimuli. J. Am. Chem. Soc. **127**, 2094–2097 (2005)

http://www.springer.com/978-981-10-5650-5

Frontiers of Quantum Chemistry

Wójcik, M.J.; Nakatsuji, H.; Kirtman, B.; Ozaki, Y. (Eds.)
2018, VIII, 512 p. 150 illus., 115 illus. in color.,
Hardcover
ISBN: 978-981-10-5650-5